ELSEVIER

Polymer 41 (2000) 6251–6262

polymer

Thermal, mechanical, physical, and transport properties of blends of novel oligomer and thermoplastic polysulfone

J.E. Robertson[a], T.C. Ward[a,*], A.J. Hill[b,c]

[a]*Departments of Chemical Engineering and Chemistry, Virginia Polytechnic Institute and State University, Blacksburg, VA 24061, USA*
[b]*CSIRO Manufacturing Science and Technology, Private Bag 33 South Clayton MDC, Victoria 3169, Australia*
[c]*Department of Chemistry, Monash University, Clayton, Victoria 3168, Australia*

Received 21 June 1999; received in revised form 3 November 1999; accepted 8 November 1999

Abstract

Thermoplastic polysulfone (PSF) was melt blended with a novel oligomer poly(bisphenol-A) (*m*-BPA) to produce samples of varying composition by weight PSF/*m*-BPA of 99/1, 95/5, 90/10, and 58/42. Miscibility studies, performed via differential scanning calorimetry and dynamic mechanical spectroscopy, show a single T_g, intermediate to the pure component T_gs, over the composition range of 1–42 wt% oligomer. Viscosity, tensile properties, moisture uptake, aging rate, specific volume, PALS free volume, and thermal stability of the blends are examined. Addition of as little as 1 wt% *m*-BPA to PSF reduces melt viscosity as measured by rheometry and causes a significant reduction in torque and RPM in the Brabender Plasti-corder. Addition of *m*-BPA to PSF causes a ductile to brittle transition in tensile properties, a decrease in relative free volume as probed by positron annihilation lifetime spectroscopy (PALS) and a decrease in water diffusion coefficient. Aging results in a decrease in the relative concentration of free volume elements for high *m*-BPA loadings. Humidity absorption produces a decrease in the relative size of free volume elements in the pure components and the blends. The thermal stability of the blends with low loadings of *m*-BPA (480–504°C) is comparable to that of PSF (499–504°C). The aging rate of the blends is intermediate to that of the pure components. © 2000 Elsevier Science Ltd. All rights reserved.

Keywords: Miscibility; Blends; PALS

1. Introduction

Use of the novel oligomer poly(bisphenol-A) (*m*-BPA) as a processing aid for high temperature thermoplastics was first reported by Robertson and Ward [1]. Addition of *m*-BPA to a polysulfone (PSF) melt causes a substantial drop in the torque and the rpm of the Brabender Plasti-corder torque rheometer. The mechanism of viscosity reduction may be related to polymer-oligomer interactions and the influence of the oligomer on free volume [2–4]. In an effort to understand the potential benefits and limitations of oligomer addition to high temperature engineering thermoplastics, and in order to further investigate the rheological effects of addition of *m*-BPA to PSF, samples were prepared over a range of compositions as well as solid state properties were measured.

The concept of utilizing oligomers as additives for polymers is not new. For example, Meng et al. [5] first synthesized a series of poly(phthalazinone ether sulfone ketone)s which proved difficult to process due to very high T_gs. In an effort to improve the processability, they then solution blended the polymers with two kinds of oligomers, a low molecular weight poly(phthalazinone ether sulfone ketone) and a commercially available poly(-ether sulfone). They reported significant decreases in melt viscosity coupled with retention of mechanical and thermal properties of the neat polymer.

Seibel and Papazoglou [6] chose oligomers as a way to increase flame retardancy in polycarbonate. They added brominated polycarbonate oligomers to bisphenol-A polycarbonate and then correlated processability and mechanical properties to the oligomer using antiplasticization theory. The authors found that tensile stiffness was improved only at high levels of oligomer addition, but rheological properties were unaffected.

Rheological properties in a polymer–oligomer system were studied by Myasnikova et al. [7] for the case of methacrylic oligomers and polymethacrylates. Schnall [8] also demonstrated the use of oligomeric additives to improve film uniformity in high-solids baking systems. In the adhesives area, oligomers have been utilized as

* Corresponding author. Tel.: +1-540-231-5876; fax: +1-540-231-8517.
E-mail address: tward@chemserver.chem.vt.edu (T.C. Ward).

0032-3861/00/$ - see front matter © 2000 Elsevier Science Ltd. All rights reserved.
PII: S0032-3861(99)00829-0

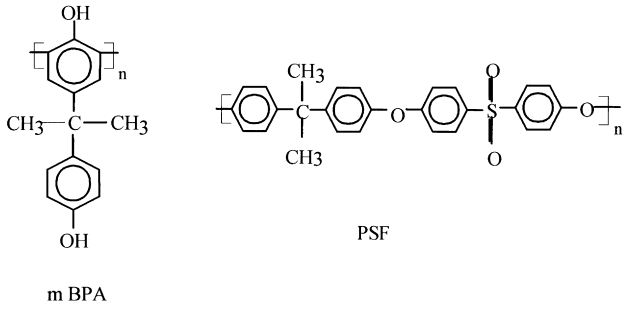

Fig. 1. Materials used in this study.

tackifiers for rubbery polymers, and it was recently shown that blend miscibility is particularly important to mechanical properties such as fracture energy, peel strength, and holding power [9].

Goldanskii et al. [10] reported on the morphology, specific volume, and PALS free volume of blends and copolymers of epoxide oligomer and metal–organic oligomer; however, these systems were thermosets and phase separated for compositions of 20 and 50 mol% oligomer. Pfau and Mayo [2] reported PALS and viscosity data for high solids coating oligomers as a function of solvent addition. Viscosity reduction was shown to be dependent on solvent type and was attributed to the effect of solvent–oligomer interaction on free volume. The PALS parameter τ_3 was used to characterize the average free volume of the solvent–oligomer systems and I_3 was used as a relative measure of the number of free volume sites. It was found that I_3 was lower for mixtures of equivalent free volume but stronger solvent–oligomer interactions. The combined effects of free volume increase with efficient disruption of oligomer–oligomer interactions in favor of solvent–oligomer interactions were suggested as responsible for viscosity reduction. Pfau and Mayo [11,12] also reported that the PALS free volume parameter τ_3 displayed lower than additive behavior over the composition range in miscible blends of polycarbonate/polycaprolactone (PC/PϵCL) and polystyrene/poly(2,6-dimethyl-1,4-phenylene-oxide) (PS/PPO). This less than additive PALS free volume behavior in miscible blends was discussed in terms of the specific interactions and volume contraction predicted by mean field thermodynamic theory [12].

The present work characterizes blends of polysulfone/*m*-BPA oligomer (PSF/*m*-BPA). In the quest for tailored properties, blending can be a cost-effective alternative to synthesizing new polymers. As polymers become more popular for use in engineering applications, the range of properties expected from these materials has never been broader. While most binary polymer systems are immiscible due to their positive free energy of mixing [13–16], there are several systems, such as PPO/PS and polystyrene/polyvinylmethylether (PS/PVME) [17] that demonstrate complete miscibility. Oligomers as blend components are the miscible example of interest to us. A full understanding of blending behavior can enable scientists and engineers to tailor properties for applications as diverse as adhesives or structural parts.

2. Experimental

2.1. Sample preparation

The materials used in this investigation are Udel™ polysulfone (PSF), provided by Amoco, and a novel oligomer, poly(bisphenol-A) (*m*-BPA). The PSF is an injection molding grade with a number average molecular weight of approximately 26,600, while *m*-BPA is an oligomeric material with number average molecular weight of 5400 and weight average molecular weight of 16,800 from our GPC analysis. The PSF molecular weight measurements were taken using an on-line viscometer, so reported quantities are absolute molecular weights. The oligomer values were taken relative to polystyrene standards. The structures of these materials are shown in Fig. 1. All materials were dried overnight in a vacuum oven to remove moisture and residual solvent, and then stored in a dessicator prior to testing. Glass transition temperatures for the neat materials were measured via differential scanning calorimetry (DSC) on a Perkin–Elmer DSC 7 at a scan rate of 10°C min^{-1}. The T_g values were found to be approximately 135°C and 186°C for *m*-BPA and PSF, respectively.

The materials were melt blended in a Brabender Plasticorder torque rheometer utilizing a 60 g mixing head. PSF was added to the blender first and allowed to melt. Then the *m*-BPA was added and the temperature lowered to prevent degradation of the oligomer. Blends with compositions of 90/10, 95/5, and 99/1 on a weight basis were prepared at temperatures of 240–280°C and about 75 rpm. Mixing times ranged from approximately 5 to 15 min, as the concentration of PSF increased. It should be noted that upon the addition of the oligomer, the torque and rpm of the melt blender dropped substantially. Torque values fell from about 1.7 N m to essentially zero. This response indicates that the oligomer may have potential as a processing aid.

It should be noted that one other blend, 58/42 PSF/*m*-BPA, was prepared under the same conditions described above. Since any oligomer would be used only at an additive level of less than a few percent, this blend was prepared purely for the purpose of elucidating miscibility. It was hypothesized that if two T_gs were present in the blends (i.e. immiscibility or partial miscibility), then having a larger concentration of the oligomer would help distinguish a second T_g. Data for this blend are not available for all tests but are included wherever applicable.

Following melt blending, samples were prepared in a Pasadena Hydraulics compression molder at 240°C and around 750 psi. The samples were left in the press for 45 minutes to one hour to let any air bubbles migrate to the

edges and to allow for sample relaxation. Unless stated otherwise, all samples were freshly quenched from T_g + 10°C (15 min anneal) and stored overnight in a vacuum oven prior to testing.

2.2. Thermal testing methods

To observe the changes in T_g, DSC was performed on each blend at a heating rate of 10°C min^{-1} from 30–250°C using a Perkin–Elmer DSC 7. Furthermore, dynamic mechanical testing was carried out on each blend as well as on neat PSF using a Netzsch DMA 242 in the dual cantilever mode. Temperatures ranged from −100 to 240°C at a heating rate of 2°C min^{-1}, an amplitude of 120 μm, and frequencies of 0.1, 0.25, 1, 5, 10, and 25 Hz. Thermogravimetric analysis (TGA) was performed on the materials in order to measure thermal stability. A DuPont Instruments 951 Thermogravimetric Analyzer was used with the temperature ramped from 30–900°C at a rate of 20°C min^{-1} in air, and weight loss was monitored.

2.3. Rheology

Rheological testing was performed on four of the blends in a Rheometrics rms 800 parallel plate rheometer. Frequency sweeps were carried out at 2% strain at a temperature of 290°C from 0.1–100 Hz. This testing temperature was chosen to reflect the temperature experienced in the Plasti-corder.

2.4. Specific density

Measurements of specific volume were made using a Micromeritics AccuPyc 1330 pycnometer. This instrument measures density by a volume displacement technique using Helium gas. Each run in the pycnometer involves five purge and fill steps, so density is measured five times. The data presented are the average of two to five such runs.

2.5. Moisture uptake

Moisture uptake behavior of the blends was also examined. Samples approximately 2×3 cm^2 and thickness 0.5–1 mm (where thickness was much less than length or width) were dried and then freshly quenched and weighed. They were then placed in water at room temperature and weight was periodically measured as a function of time using a Mettler AE200 analytical balance. Using Fick's law to fit the data, values were obtained for the diffusion coefficient and the equilibrium mass uptake. In addition, humidity absorption was calculated by exposing samples to 23°C and 50% relative humidity (RH) and subsequently measuring the weight loss on evacuation for 48 h in a vacuum oven at 37°C.

2.6. Positron annihilation lifetime spectroscopy

Measurements of PALS parameters were made using an automated EG&G Ortec fast-fast coincidence apparatus temperature stabilized at 23°C. The source consisted of 1.3 MBq of ^{22}NaCl deposited on Ti foil and sandwiched between identical samples of 1.3 mm thickness. This source gave a single component (~167 ps) fit to annealed aluminium; hence no source correction was used in the analysis of the data using the PFPOSFIT program [18]. The spectra were modeled as the sum of three decaying exponentials; only the third component (τ_3, I_3) showed systematic variation with composition and will be reported. The PALS results did not vary as a function of contact time with the ^{22}Na source. From seven to nine spectra were collected for each sample, and the results are the mean values with error bars based on population standard deviation. Samples were measured in quenched and aged conditions (i) in ambient air (22°C, 50% RH); (ii) in ultra-dry nitrogen; and (iii) post-vacuum anneal (25 in Hg, 37°C for 48 h) in ultra-dry nitrogen. The aged samples were prepared by storage for 6 months in ambient conditions.

2.7. Dynamic mechanical testing

In order to observe potential changes in the sub T_g transitions, further dynamic mechanical analysis was performed on a Seiko DMS 210. Samples of 2 mm^2 cross-section and long enough for a 10 mm clamping length were run in tension at 2°C min^{-1} from −150 to 50°C at 0.1, 0.3, 1, 3, 10, and 20 Hz.

2.8. Mechanical testing

Mechanical properties of the blends were measured using a Polymer Laboratories Miniature Materials Tester (minimat). Samples were cut using an ASTM D3368 dogbone die such that the width was 3 mm and the gauge length was 1 cm. Thicknesses varied from 0.5–1 mm. Each specimen was pulled at a rate of 5 mm min^{-1} to a maximum load of 200 N and up to 20 mm displacement to generate a stress–strain curve. Tensile modulus, yield strength, and toughness (or strain energy) from the area under this curve, were calculated.

2.9. Physical aging

Physical aging rate measurements were carried out in the Perkin–Elmer DSC 7. Each sample was taken above T_g for 15 min to erase any thermal history and then quenched to room temperature at a rate of 200°C min^{-1}. Next, the material was taken to a temperature 14.5°C below the T_g for that blend composition and held for 0.1, 0.3, 1, 3, 10, and 30 h. Then it was again quenched and scanned at a rate of 10°C min^{-1}. After once again erasing thermal history, the sample was scanned at 10°C min^{-1} to obtain the unaged heat capacity. For each blend composition, a single sample was utilized for each of the six aging times.

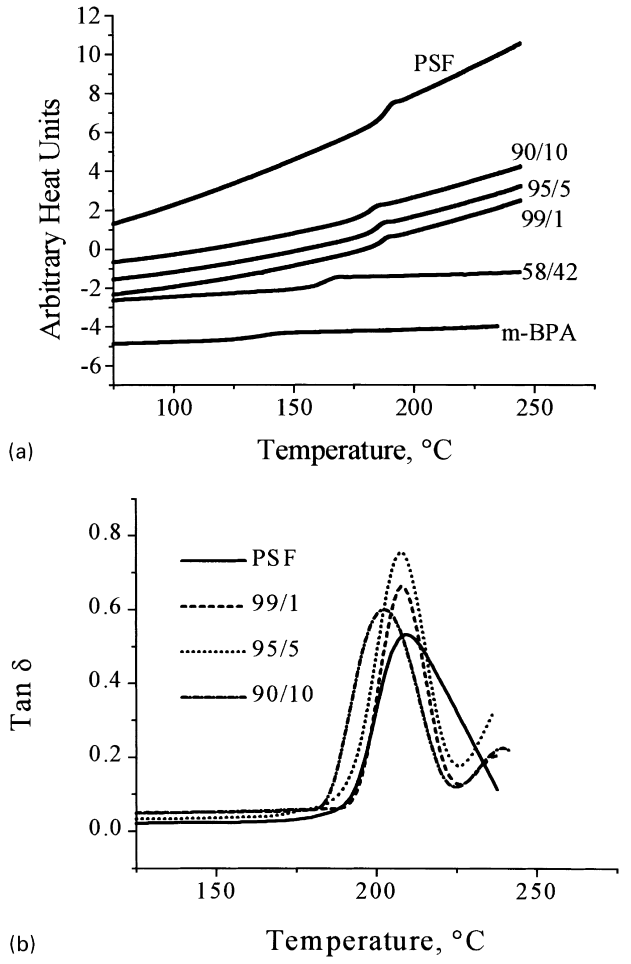

Fig. 2. (a) DSC scans of all blends indicating single T_g and hence miscibility. (b) DMTA data for some of the blends demonstrating a single T_g and hence miscibility.

3. Results

3.1. Miscibility

It is well accepted that the presence of a single T_g in a blend is indicative of miscibilty for that system [13,14]. Based on data from DSC and dynamic mechanical tests, a single T_g is observed for each of these blends (Fig. 2a and b) indicating full miscibility over the composition range under investigation. Further, this observed T_g is intermediate to the T_gs of the neat components and is approximately given by the Fox equation with mass fractions w_i [19]:

$$\frac{1}{T_g} = \frac{w_1}{T_{g1}} + \frac{w_2}{T_{g2}} \quad (1)$$

or by Couchman's equation with masses m_i [20]

$$\ln T_g = \frac{m_1(\Delta C_{p_1}) \ln T_1 + m_2(\Delta C_{p_2}) \ln T_2}{m_1(\Delta C_{p_2}) + m_2(\Delta C_{p_2})} \quad (2)$$

with $\Delta C_{p1} = 0.222$ J/(g °C) and $\Delta C_{p2} = 0.305$ J/(g °C). One should note the difficulty in obtaining an accurate value for ΔC_{p2} if there is a relatively small heat capacity step, as was the case for the oligomer of our study. Therefore, it is uncertain how much error exists in the T_g value calculated from the Couchman method. The data in Table 1 compare the measured and calculated T_g values (Eqs. (1) and (2)).

3.2. Oxidative behavior

Udel has many applications as a high use temperature material. Furthermore, the hydroxyl groups on the oligomer should impart antioxidant behavior to this material [21] and promote thermal stability. It is thus of interest to examine the high temperature behavior of the Udel blends. As seen in Table 1, the oligomer depresses the 5% weight loss temperature slightly relative to the neat PSF. However, the blends are still thermally stable to about 480°C, adequate for most applications.

3.3. Rheology

Since the processing of any thermoplastic is largely a matter of the melt viscosity, frequency sweeps were performed on four of the blends to quantify the effect of oligomer on rheology. The data were then normalized by the viscosity of the neat PSF in order to more clearly quantify how the oligomer affects the blend. These results are illustrated in Fig. 3.

Clearly, the 25% decrease in viscosity upon addition of oligomer to PSF does not account for the large drop in torque observed during melt blending. However, it should be noted that the rheometer conditions of 100 Hz and 2% strain are less vigorous than actual conditions encountered during processing in the Brabender. Under more severe conditions, shear thinning could be more pronounced,

Table 1
Oxidation and DSC T_g results for blends

Melt blend composition	5% Weight loss (°C)	T_g onset (°C)	Predicted T_g (°C) [Fox Eq. (1)]	Predicted T_g (°C) [Couchman, Eq. (2)]
PSF	499–504	186	–	–
99/1	502–504	183	185	185
95/5	494–495	182	183	182
90/10	480–489	179	180	179
58/42	407	160	163	160
m-BPA	348	135	–	–

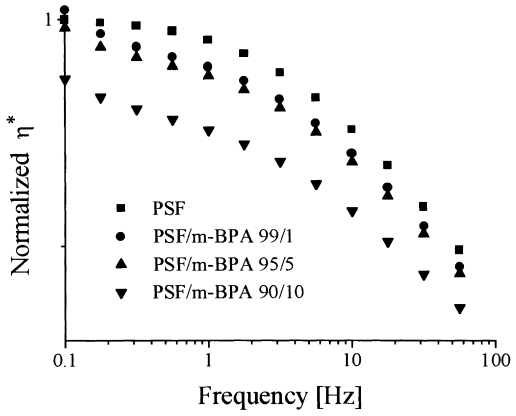

Fig. 3. Frequency sweeps for four of the blends at 290°C and 2% strain.

leading to a lower viscosity for the blends containing more oligomer. At present, this explanation remains a hypothesis.

3.4. Pycnometry data

Fig. 4 shows the results of the pycnometry testing. The data are shown in terms of the specific volume. The dotted line indicates the result expected from linear additivity. Within experimental error, the blend specific volumes display approximately linear additivity with composition except for the 58/42 blend which shows less then volume additivity. This behavior at 42 wt% *m*-BPA may be due to some interactions between PSF and the oligomer which cause the chains to pack more closely than additivity would suggest. Thus, at higher oligomer loading levels, the behavior of the blend is consistent with a miscible system.

3.5. PALS and moisture uptake

Positron annihilation lifetime spectroscopy (PALS) examines free volume from a more molecular perspective. Semi-empirical equations relating orthoPositronium (oPs) lifetime τ_3 to free volume cavity size have been developed for spherical, ellipsoidal, and cuboidal cavities [22–24].

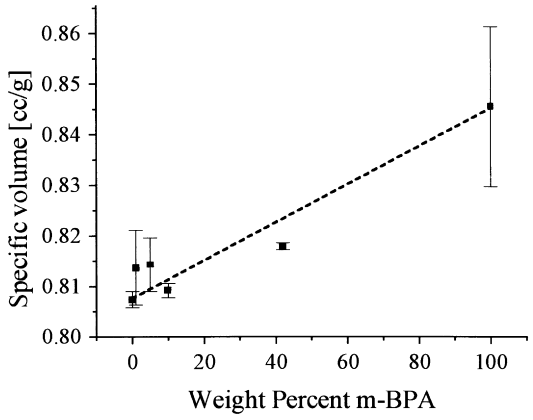

Fig. 4. Pycnometry data for the blends. Line drawn to indicate additivity.

These equations are not intended to be quantitative; but, the qualitative changes in oPs lifetime reflect qualitative changes in the characteristic length, l_c, of free volume cavities (radius, cuboid side) [23]. Over the range of lifetimes (1–3 ns) typically measured for polymers, one can approximate $\tau_3 \propto l_c$, such that volume of the cavities, $V \propto (l_c^3$, scales with τ_3^3. In the absence of oPs inhibition [25], the statistical weight I_3 is representative of the relative concentration of free volume cavities.

The data in Fig. 5a and b for quenched and aged samples at ambient conditions lead to several observations. Addition of *m*-BPA to PSF decreases the mean free volume cavity size, τ_3, but the relative number of cavities, I_3, remains approximately constant for additions up to 10 wt%. The relative free volume concentration as indicated by I_3 decreases for oligomer additions greater than 10 wt% and decreases with aging in the high *m*-BPA containing samples. This reduction in I_3 on aging is consistent with results reported for aging of glassy bisphenol-A polycarbonate [26–29]. The less than additive τ_3 behavior with composition is observed for both quenched and aged samples and may be reflecting the miscibility [11,12].

Figs. 6a and b consider the effects of moisture uptake on the PALS free volume parameters. Moisture uptake, for samples exposed at 23°C to 50% RH, causes a decrease in τ_3 with little or no effect on I_3. The data in Fig. 6a and b compare samples with ambient moisture content (humidity absorption as per Table 2), to similar samples exposed to ultra-dry nitrogen, and to similar samples evacuated for 48 h in the vacuum oven and exposed to ultra-dry nitrogen. Ultra-dry nitrogen exposure increases τ_3 by 0.02 ns whilst vacuum oven plus ultra-dry nitrogen causes an increase in τ_3 of 0.04 ns. Thus, humidity absorption in the PSF/*m*-BPA system results in a decrease in the mean free volume cavity size, τ_3, as measured by PALS.

Because PSF is known to absorb significant amounts of moisture, and because the oligomer has two pendant hydroxyl groups on each repeat unit, the moisture uptake behavior of these blends was of interest. Using the technique outlined in the Section 2, and fitting the moisture uptake data (see Fig. 7) to Fick's Law, a diffusion coefficient, D, and an equilibrium mass uptake, m_∞, were measured for freshly quenched samples as shown Fig. 8a and b. One should note here each value is the average over two samples. Errors associated with the diffusion coefficient are on the order of 5×10^{-11}, smaller than the size of the data points in Fig. 8b, and as such are not shown on the graph. The general trend is a decreasing *D* and an increasing m_∞ with added oligomer. We should expect increases in m_∞ since, as more oligomer is added, there are more sites to which water can bind. A decreasing *D* value indicates that water diffuses more slowly as more oligomer is present. The moisture absorption was also measured for samples exposed to 50% RH at 23°C and the trend is similar to that found for equilibrium mass uptake (samples immersed in water) as shown in Table 2.

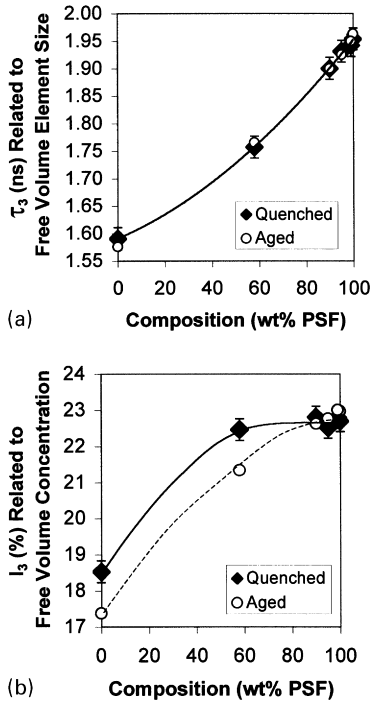

Fig. 5. (a) oPs pickoff lifetime τ_3, related to free volume cavity size, plotted as a function of composition for quenched and aged samples. Line drawn to indicate trend. (b) oPs pickoff intensity, I_3, related to free volume concentration, plotted as a function of composition for quenched and aged samples. Lines drawn to indicate trends.

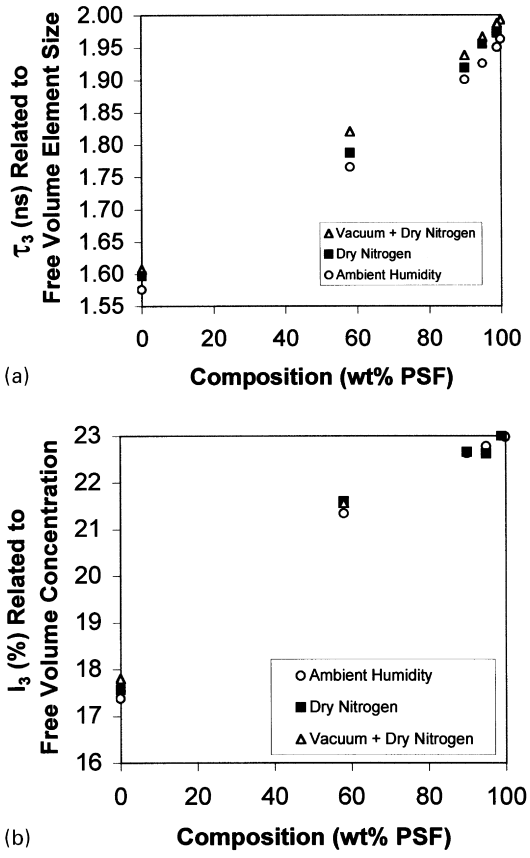

Fig. 6. (a) oPs pickoff lifetime τ_3, related to free volume cavity size, plotted as a function of composition for dry, moisture saturated and intermediate samples. (b) oPs pickoff intensity, I_3, related to free volume concentration, plotted as a function of composition for dry, moisture saturated and intermediate samples.

3.6. Secondary transition and tensile behavior

The PALS free volume and moisture absorption data suggested a reduction in molecular mobility on addition of *m*-BPA to PSF. The behavior (magnitude, breadth, activation energy) of the secondary transition, (termed γ), can be used as a measure of molecular mobility [30]. Boyer and other workers [31,32] have theorized that prominent secondary transitions in some polymeric materials contribute to their tough behavior. PSF exhibits a γ transition and is generally thought of as a tough resin. The behavior of the secondary transition as a function of oligomer content in the blends was of interest in order to determine its role in transport and mechanical properties. For each blend, data from all frequencies were fit to an Arrhenius expression to calculate the activation energy for the γ transition. In Table 3, one can see that the activation energy showed no change with oligomer content. Each datum, except the 5 wt% value, represents a single sample tested at several frequencies. Thus the error for these points come from the error in the linear fit to the Arrhenius equation. At 5 wt%, however, three separate samples were tested at all frequencies, so the error here reflects the population standard deviation. This larger error gives an indication of the accuracy of this method, which, like all mechanical tests, is affected greatly by any sample imperfections. The constancy of activation energy for this system indicates that the γ transition is not shifting or being obscured by the oligomer. In Fig. 9, we see that neat PSF exhibits significant yielding and hence toughness (or ductile failure). With only 1 wt% oligomer added, however, yielding behavior is suppressed, and the material shows only brittle failure.

Table 2
Humidity absorption for blends

Melt blend composition	Humidity absorption (wt%)
PSF	0.1
99/1	0.4
95/5	0.6
90/10	0.5
58/42	0.7
m-BPA	1.1

3.7. Physical aging

Over the application lifetime of a material, physical changes can occur which affect dimensional stability as well as mechanical properties. To see how the presence of the oligomer could affect the long-term engineering performance of PSF, physical aging studies were conducted.

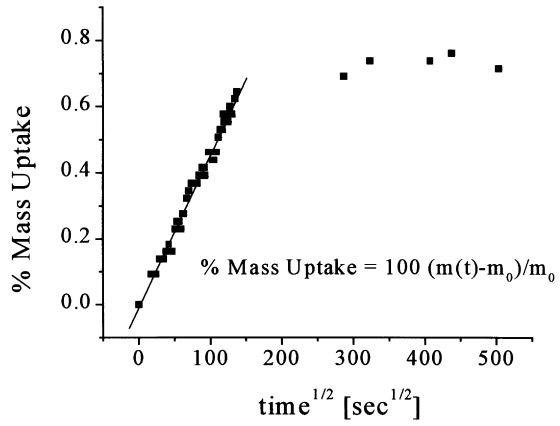

Fig. 7. Representative moisture uptake versus time graph for neat PSF.

Using the DSC data as described in the experimental section, the enthalpy recovery following isothermal annealing can be calculated from the difference in heat capacity between the aged and unaged sample. For each blend, this change in heat capacity was plotted versus log aging time, forming a straight line. The slope of this line was then defined as the aging rate. Fig. 10 shows raw data for the 95/5 blend, which is representative of all the blends, while Table 3 tabulates the values for the aging rates for each composition.

As expected, the longer aging times in Fig. 10 show a higher heat capacity overshoot at T_g which is characteristic of physical aging. The general trend in rates of aging, shown in Table 3, is their increase with increased amounts of oligomer. These data are measured at $T_g - 14.5$°C. The samples with the highest aging rates, *m*-BPA and the 58/42 blend, exhibited a decrease in the relative free volume concentration, I_3, during aging at 23°C over a six month period. If the PSF/*m*-BPA blends were to be used in an application, more attention would have to be placed on the aging characteristics since the oligomer appears to accelerate the aging rate.

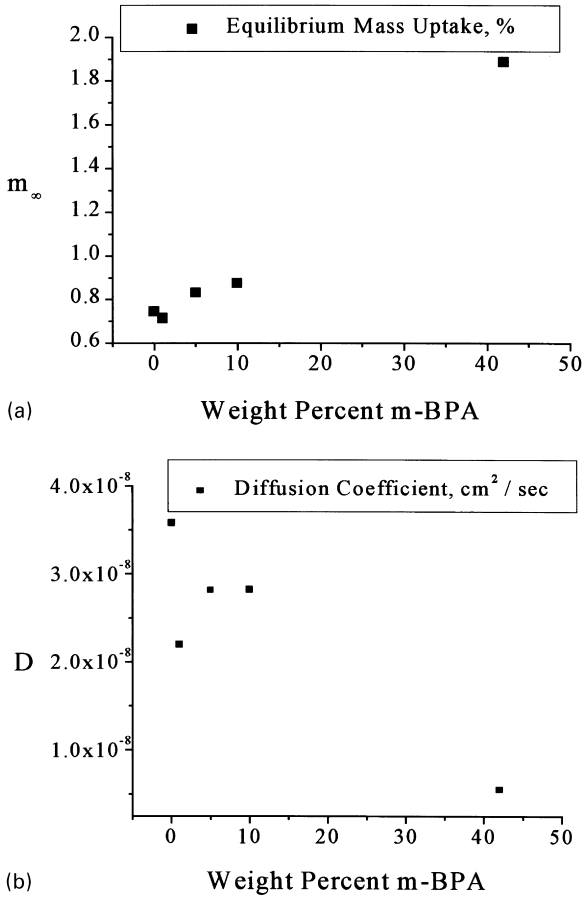

Fig. 8. (a) Water absorption results for PSF and blends. (b) Diffusivity of water in PSF and blends.

4. Discussion

From the above results, miscibility is clearly indicated for this blend. While one can speculate on the mechanism of this miscibility, no definitive answers are evident from the T_g data. When the Fox equation is used, the measured T_gs are slightly less than predicted by approximate volume (or free volume) additivity of the components [33]. This negative deviation of T_g from free volume additivity could indicate weak specific interactions between the components [34]. Schneider [33] has suggested that this T_g behavior results from binary hetero-contact formation within the blends leading to local interchain orientation. The smaller the induced local orientation, the larger the mobility, conformational entropy changes, and free volume (and hence lower T_g than predicted). Thus the glass transition data could suggest that weak oligomer–polymer interactions are resulting in "looser" packing at T_g than predicted by free volume additivity [33].

If the Couchman equation is applied to the T_g data, however, no negative deviation from additivity is observed, since measured values closely match those calculated. However, there was difficulty in obtaining an accurate value for ΔC_{p2} due to the small change in the heat capacity change for the oligomer. For these calculations, a value of 0.305 J/(g °C) was used for ΔC_{p2} while ΔC_{p1} was taken as 0.222 J/(g °C). Due to the aforementioned problems, it was not possible to estimate error in this calculation.

It should be pointed out that Fourier Transform Infrared Spectroscopy (FTIR) was applied to these samples to interrogate any specific interactions. However, difficulties were encountered in examining the peak associated with the hydroxyl group. Even though samples were dried prior to testing, it was unclear whether slights shifts observed in this region were due to interactions between the polymer and oligomer, or to moisture uptake since this region would also correspond to water in the samples. Both components are quite hydrophilic, and they were inevitably subjected to environmental humidity for short times just prior to testing. No conclusions could be drawn from these tests.

Table 3
Aging rate and secondary transition results

Composition	Aging rate ($J\ g^{-1}$ decade^{-1}) (standard deviation)	Activation energy for γ transition ($kJ\ mol^{-1}$) (standard deviation)
PSF	0.81 (0.02)	53.3 (1.4)
99/1	–	52.6 (1.4)
95/5	0.86 (0.02)	53.9 (6.7)
90/10	0.86 (0.04)	52.7 (1.4)
58/42	0.88 (0.05)	–
m-BPA	1.17 (0.07)	–

Examination of the rheological data provides additional insight regarding the miscibility. Utracki et al. [35] noted that for blends with specific interactions leading to miscibility, there is frequently a positive deviation of measured viscosity for the blend from that calculated from viscosities of the neat resin. By plotting $\ln(\eta_0)$ versus weight fraction oligomer one can examine whether specific interactions play a role in the miscibility of the PSF/*m*-BPA system. Such a plot is displayed in Fig. 11 where zero-shear viscosity (η_0 derived from the low frequency data of Fig. 3) is shown for neat PSF and the 99/1, 95/5, and 90/10 blends. Obtaining viscosity data for the neat oligomer at 290°C was not possible. As frequency is increased, in Fig. 3, the viscosity is reduced and the addition of oligomer causes further viscosity reduction (suggesting an increase in system free volume). However, at the lowest frequency, one can clearly see that addition of the oligomer leads to a positive deviation from additivity for this system (Fig. 11), implying that there are specific interactions in this miscible system leading to free volume reduction. Thus, the free volume trend with oligomer addition (less than, greater than, or additive with composition), as inferred from the melt properties of this blend system, appears to be a function of the measurement temperature. This finding is discussed further in the final section of the discussion.

Since free volume changes are believed to be important in this system, it was of interest to carry out some related

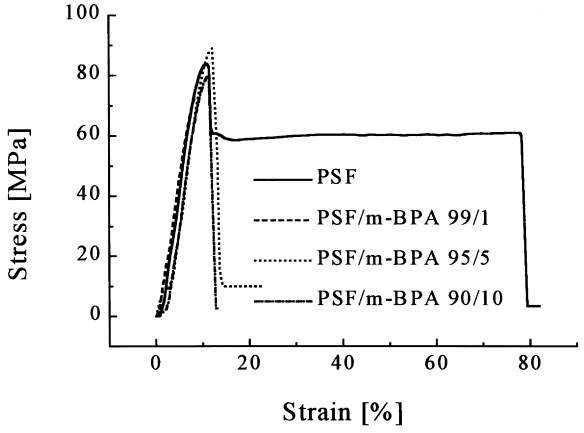

Fig. 9. Results of tensile testing for some of the blends.

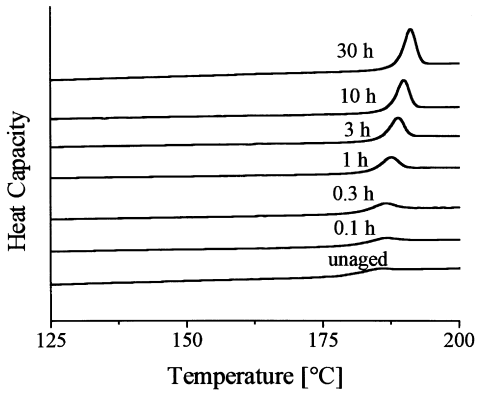

Fig. 10. Aging data for 95/5 blend.

calculations. The fractional free volume (FFV) calculated using the group contribution method of Bondi [36] is most often used to characterize solid state chain packing [37]. The FFV is defined as

$$\mathrm{FFV} = (V - V_o)/V \tag{3}$$

where V is the specific volume and V_o is the occupied volume of the polymer. The occupied volume can be estimated as 1.3 times the van der Waals volume of the constituent monomers [38]. Calculations using Eq. (3) give values of FFV ranging from 0.10 for *m*-BPA to 0.15 for PSF as shown in Fig. 12. Eq. (3) gives information on the total amount of free volume but does not indicate its size distribution.

Recent evidence [39–42] suggests that PALS data can be utilized to model water absorption and free volume changes in polymeric materials. Several researchers [40–42] have shown that moisture absorption in nylon-6 is accompanied by an initial decrease in τ_3. PALS results for nylon-6 [40–42] are shown in Fig. 13a and b. During initial water absorption τ_3 decreases and I_3 decreases, and this response correlates with absorption of strongly bound water molecules

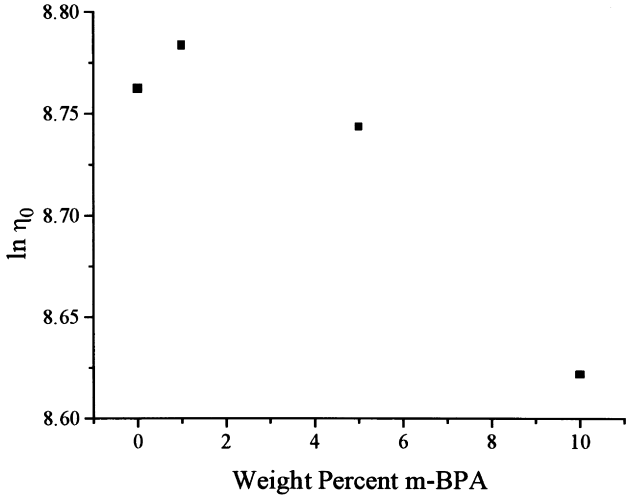

Fig. 11. Zero-shear-rate viscosity versus weight percent *m*-BPA for blends.

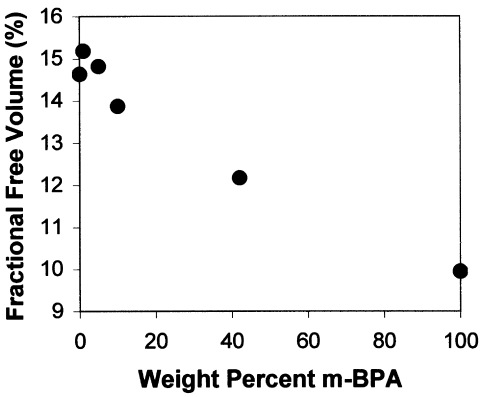

Fig. 12. Fractional free volume calculated by group contribution method.

hydrogen bonding the N–H and C=O groups [43]. These water–polymer interactions lead to occupation of free volume, as evidenced by PALS, and by modulus and transport results [40–45]. Heater [40] proposed a hole-filling mechanism whereby molecular water enters a free volume cavity and effectively decreases the cavity size. The free volume cavity size, as represented by τ_3, begins to increase when water pushes the chains apart due to plasticization/swelling of the polymer. As shown in Fig. 6a, the τ_3 values

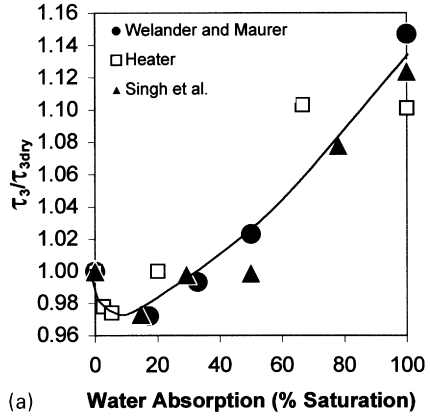

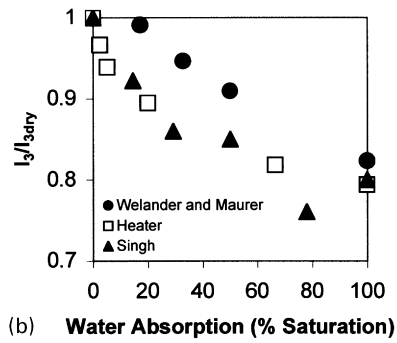

Fig. 13. (a) Normalized oPs pickoff intensity data for nylon-6 as a function of water absorption. Weight percent water absorption is normalized to percentage of saturation. (b) Normalized oPs pickoff intensity data for nylon-6 as a function of water absorption. Weight percent water absorption is normalized to percentage of saturation.

for the PSF/*m*-BPA system decrease with equilibrium moisture absorption. It thus appears that PSF/*m*-BPA samples exposed to ambient humidity are in the initial hole filling stage prior to swelling.

The PALS data in Figs. 5 and 6 show that τ_3 is less than additive with composition in contrast to I_3 which is approximately constant for oligomer additions up to 10 wt%. These results are is independent of whether the samples are quenched or aged and whether they contain ambient moisture content or are dry. The data suggest that small additions (<10 wt%) of *m*-BPA to PSF decrease the molecular free volume by reducing the mean free volume cavity size. This result can be compared to the fractional free volume, FFV, calculated from specific volume and group contribution methods [37–38] which shows greater than additive values for 1 and 5 wt% additions of *m*-BPA and less than additive values for 10 wt% (Fig. 12). The discrepancy between the PALS free volume and density-based free volume may be attributed to many factors, including the effect of macroscopic defects on density. In addition, oPs probes only submicroscopic free volume cavities that are accessible to it on a size and frequency basis [46]. Both PALS and density-based FFV indicate that free volume is decreased on going from neat PSF to neat *m*-BPA. This reduction in total free volume should be reflected in penetrant transport properties.

The moisture uptake results are consistent with the PALS free volume results. Reduction in τ_3 on addition of *m*-BPA to PSF indicates a reduction in the accessible free volume such that diffusive jumps are less probable. This effectively makes it more difficult for water to move within the blend, leading to a longer time scale for diffusion. The modeling work of Greenfield and Theodorou [47] suggests that a penetrant molecule of sufficiently large radius sorbed at low concentration within a glassy polymer spends most of its time confined in small disjoint clusters of accessible free volume. Transient connecting passages that open nearby due to thermal fluctuations allow diffusive jumps from cluster to cluster. This "Red Sea" mechanism has been shown to prevail for diffusion of water in poly(vinyl alcohol) (PVOH) by Müller-Plathe [48]. The addition of *m*-BPA to PSF lowers the PALS free volume in a similar manner to that shown by the addition of the stiff 2,6-napthalene (N) units of poly(ethylene napthalate) (PEN) to poly(ethylene terephthalate) (PET) [49]. The addition of naphthalene by copolymerization of PET with PEN results in a decrease in diffusivity and PALS free volume even though m_∞, the equilibrium value, (and hence sorption) increases [49–50].

It is of interest to compare the penetrant transport and PALS free volume responses for the three cases discussed in the previous paragraph, namely, (i) blending of *m*-BPA with PSF, (ii) plasticization of PVOH by water, and (iii) copolymerization of PET with PEN. The equation of Cohen and Turnbull [51],

$$D = B\exp(-C/V_f) \tag{4}$$

where D is diffusivity, B and C are constants, and V_f is the

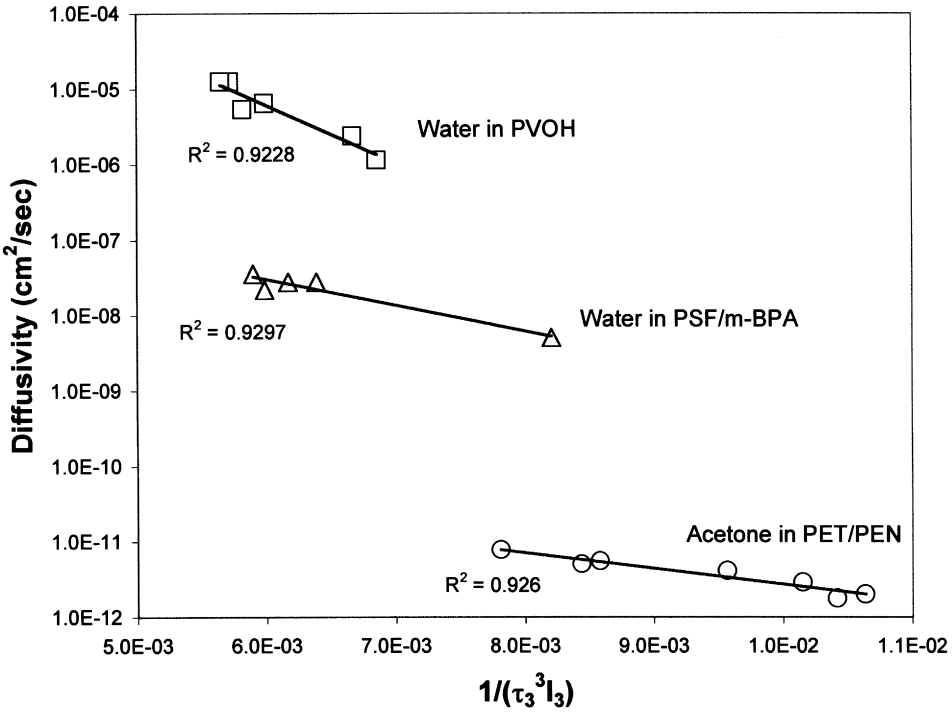

Fig. 14. Comparison of the relationship between diffusivity and PALS free volume for water in PVOH [43], acetone in PET/PEN copolymers [44], and water in PSF/*m*-BPA blends.

average free volume available for diffusive jumps, allows evaluation of the relationship between free volume and diffusivity. Eq. (4) predicts a linear relationship between $\ln(D)$ and V_f^{-1}, and it has been previously shown that the PALS parameter $\tau_3^3 I_3$ can be used to represent the average free volume V_f [52]. Fig. 14 compares a plot of $\ln(D)$ versus $(\tau_3^3 I_3)^{-1}$ for the three cases. In these cases the reasonable fits to these data indicate that the oPs probes the same static and dynamic free volume cavities accessible to the penetrant molecules. These room temperature data suggest that the tighter molecular packing and specific interactions that occur on addition of *m*-BPA to PSF restrict the molecular fluctuations necessary for the opening of transient passages.

Mechanical behavior of this blend system, particularly toughness, is of prime importance for any future applications of the materials. For PSF, it has been observed that addition of even 1 wt% oligomer leads to brittle failure. This feature, which has been previously reported in miscible blends [16], can be explained by considering the loss of free volume mentioned above. When energy is introduced into a sample via some mechanical test, there must be some mechanism for dissipation of this energy, which is frequently reptation of the chains. With less free volume in the blends, there is also less chain mobility, which means energy cannot be effectively dissipated, resulting in brittle failure. Due to the lack of change in the γ transition, it is likely that this secondary transition does not play a vital role in the free volume and mobility reduction responsible for the transport and mechanical properties.

5. Free volume

In the present work we have studied numerous phenomena that are modeled using free volume theory: (i) viscosity [53]; (ii) blend miscibility [54]; (iii) the glass transition [55]; (iv) plasticization [56]; (v) penetrant transport [51]; (vi) the ductile to brittle transition [57]; and (vii) physical aging [58]. The results for each of these phenomena in the PSF/*m*-BPA system are consistent with free volume theory, and here the room temperature properties correlate well with the room temperature free volume measurements. However, the glass transition and melt properties indicated an enhanced free volume on addition of oligomer to PSF (reduced viscosity, negative deviation of T_g from additivity) whilst the room temperature properties of the blends indicate a reduction in free volume (embrittlement, reduced diffusivity). The room temperature free volume size distribution, as probed by PALS, shows that the mean free volume cavity size, represented by τ_3, decreases on addition of oligomer to PSF. The relative concentration of free volume cavities, I_3, does not decrease until an amount greater than 10 wt% of oligomer is added to PSF. PALS data were not measured in the glass transition temperature range (136–186°C) or at the viscosity measurement temperature (290°C).

Specific volume measurements of Zoller and Hoehn [59] for the miscible blend system PS/PPO show less than additive specific volume at room temperature and additive specific volume in the supercooled liquid (well above T_g). Similarly, Li et al. [60] have measured PALS free volume in miscible PS/poly(phenylene ether) blends at room

temperature, T_g, and $T_g + 50°C$. They have observed variations in the free volume behavior of the blend system:(τ_3 is less than additive with composition at 25°C and additive with composition at T_g and $T_g + 50°C$. Robertson [61] has interpreted these temperature dependent volume-versus-composition trends in terms of the influence of intermolecular interactions on relaxation time and molecular packing. A similar interpretation may be applicable to the liquid and glassy state data presented in the current work. Specific volume and PALS free volume measurements in the glass transition and liquid regions of this blend system are left for future work.

6. Conclusions

Blends of the oligomer *m*-BPA with Udel™ PSF have been investigated by a variety of methods, focussing on the effect of small additions of oligomer on the rheological, physical, transport, thermal, and mechanical properties. The large drop in torque and the rpm observed during blending is present only under conditions of extreme shear such as that found in the Brabender Plasti-corder and could not be reproduced in a parallel plate rheometer although some viscosity reduction was observed. Although the glass transition and melt properties indicate an increase in free volume on addition of *m*-BPA ($M_n = 5400$) to PSF ($M_n = 26,600$), the room temperature properties of the blends indicate a reduction in free volume. The molecular level free volume was measured by PALS at room temperature and shows a decrease in the mean free volume cavity size on addition of *m*-BPA to PSF. The relative concentration of free volume cavities is reduced only for oligomer additions greater than 10 wt%. The blends appear miscible (single T_g) over the composition range investigated. A reduction in free volume occurred on ambient absorption of moisture and was attributed to partial filling of free volume sites without expansion of intermolecular distances. A reduction of free volume occurred on room temperature aging of the higher *m*-BPA containing samples. Aging rate was shown to increase on addition of *m*-BPA to PSF. PSF was embrittled by the addition of as little as 1 wt% *m*-BPA although there was no effect on the sub-T_g γ relaxation. Embrittlement and reduction in water diffusivity were attributed to polymer–oligomer interactions and reduced free volume cavity size on addition of *m*-BPA to PSF. The oxidative resistance of PSF is only slightly reduced on addition of *m*-BPA, and the benefits of *m*-BPA as a processing aid are substantial [1]. However, these benefits may be outweighed by the ductile to brittle transition caused by the addition of *m*-BPA to PSF.

Acknowledgements

The authors would like to thank Amoco for donation of materials. Financial support of the NSF Science and Technology Center at Virginia Tech, Contract no. DMR-9120004, is also greatly appreciated. Dr K.J. Heater is thanked for allowing the publication of his data for nylon-6.

References

[1] Robertson JE, Ward TC. Society of Plastics Engineers ANTEC 1998;II:2524.
[2] Pfau JP, Mayo BA. Polym Mater Sci Engng 1987;46:749.
[3] Doolittle AK. The technology of solvents and plasticisers, New York: Wiley, 1954.
[4] Wick ZW. J Coatings Technol 1986;58:22.
[5] Meng YZ, Hay AS, Jian XG, Tjong SC. J Appl Polym Sci 1997; 66:1425.
[6] Seibel SR, Papazoglou E. Society of Plastics Engineers ANTEC 1995;I:366.
[7] Myasnikova LI, Yemel-yanov DN, Irzhak VI, Panova GD, Bogdanova LM. Polym Sci USSR 1987;29:1039.
[8] Schnall MJ. J Coatings Technol 1992;64:77.
[9] Kim H-J, Hayashi S, Mizumachi H. J Appl Polym Sci 1998;69:581.
[10] Gol'danski AV, Zherdev V, Shantarovich VP, Onishchuk VA, Zalavskii BI, Sipyagina MA, Stepanova EE, Klochkov AA. Plaste Kautsch 1985;32:451.
[11] Pfau JP, Mayo BA. Polym Mater Sci Engng 1988;59:273.
[12] Mayo BA, Pfau JP. In: Carrillo G, Newell ED, Brown WD, Phelan P, editors. Materials-pathway to the future, Thirtythird International SAMPE Symposium, SAMPE, Covina CA, 33, 1988. p. 1751–60.
[13] Paul DR, Sperling LH, editors. Multicomponent polymer materials Advances in chemistry series, 211. Washington, DC: ACS, 1986.
[14] Utracki LA. Polymer alloys and blends: thermodynamics and rheology, Munich: Hanser, 1989.
[15] Sanchis A, Masegosa RM, Rubio RG, Prolongo MG. Eur Polym J 1994;30:781.
[16] Zipper MD, Simon GP, Tant MR, Small JD, Stack GM, Hill AJ. Polym Int 1995;36:127.
[17] Abtal E, Prud'homme RE. Macromolecules 1994;27:5780.
[18] Puff W. Comput Phys Commun 1983;30:359.
[19] Fox TG. Bull Am Phys Soc 1956;1:123.
[20] Couchman PB. Phys Lett 1979;70A:155.
[21] Pospíšil J. In: Scott G, editor. Developments in polymer stabilisation, 1. London: Applied Science Publishers, 1979. p. 1.
[22] Nakanishi H, Wang SJ, Jean YC. In: Sharma SC, editor. International symposium on positron annihilation studies of fluids, Singapore: World Scientific, 1987. p. 292.
[23] Jasinska B, Koziol AE, Goworek T. J Radioanal Nucl Chem 1996;210:617.
[24] Jean YC, Shi H. J Non-Cryst Solids 1994;172–4:806.
[25] Ito Y, Tabata Y. In: Ache HJ, editor. Positronium and muonium chemistry, Advances in Chemistry Series, 175, 1979. p. 109 Chap. 5.
[26] Hill AJ, Jones PJ, Lind JH, Pearsall GW. J Polym Sci A: Polym Chem 1998;A26:1541.
[27] Heater KJ, Jones PL. In: Roe RJ, O'Reilly JM, editors. Structure, relaxation, and physical aging of glassy polymers, MRS symposium proceedings, 215, 1990. p. 207.
[28] Kluin JE, Yu Z, Vleeshouwers S, McGervey JD, Jamieson AM, Simha R, Sommer K. Macromolecules 1853:26.
[29] Davis WJ, Pethrick RA. Eur Polym J 1998;34:1747.
[30] Kim CK, Aguilar-Vega M, Paul DR. J Polym Sci B: Polym Phys 1992;30:1131.
[31] Boyer RF. Polym Engng Sci 1968;8:161.
[32] Hartmann B, Lee GF. J Appl Polym Sci 1979;23:3639.
[33] Schneider HA. J Res Natl Inst Stand Technol 1997;102:229.
[34] Chee KK. Polymer 1995;36:809.
[35] Utracki LA, Walsh DJ, Weiss RA. In: Utracki LA, Weiss RA, editors. Multiphase polymers: blends and ionomers, ACS Symposium Series-Washington, DC: ACS, 1989. p. 1.

[36] Bondi A. J Phys Chem 1964;68:441.
[37] Ghosal K, Freeman BD. Polym Adv Technol 1994;5:673.
[38] Van Krevelen D. Properties of polymers. Elsevier, Amsterdam 1990:875.
[39] Soles CL, Chang FT, Bolan BA, Hristov HA, Gidley DW, Yee AF. J Polym Sci B: Polym Phys 1998;36:3035.
[40] Heater KJ, McDonald WF. Proceedings of 1992 ASNT Spring Conference, Orlando, FL, 30 March–3 April, 1992, p. 175.
[41] Welander M, Maurer FHJ. Mater Sci Forum 1992;105–10:1815.
[42] Singh JJ, St Clair TL, Holt WH, Mock W. Nucl Instrum Meth Phys Res 1984;221:427.
[43] Khanna YP, Day ED, Tsai ML, Vaidyanathan G. J Plastic Film Sheeting 1997;13:197.
[44] Starkweather Jr HW. In: Koham MI, editor. Nylon plastics, New York: Wiley, 1973. p. 323.
[45] Deopura BL, Sengupta AK, Verma A. Polym Commun 1983;24:287.
[46] Hill AJ, Zipper MD, Tant MR, Stack GM, Jordan TC, Shultz AR. J Phys: Condens Matter 1996;8:3811.
[47] Greenfield ML, Theodorou DN. Macromolecules 1993;26:5461.
[48] Muller-Plathe F. J Membrane Sci 1998;141:147.
[49] McDowell CC, Freeman BD, McNeely GW, Haider MI, Hill AJ. J Polym Sci B: Polym Phys 1998;36:2981.
[50] Rueda DR, Varkalis A. J Polym Sci B: Polym Phys 1995;33:2263.
[51] Cohen MH, Turnbull D. J Chem Phys 1959;31:1164.
[52] Hill AJ, Weinhold S, Stack GM, Tant MR. Eur Polym J 1996;7:843.
[53] Doolittle AK. J Appl Phys 1951;22:1471.
[54] Patterson D, Delmas G. Trans Faraday Soc 1969;65:708.
[55] Cohen MH, Turnbull D. J Chem Phys 1961;34:120.
[56] Maeda Y, Paul DR. J Polym Sci B: Polym Phys 1987;25:1005.
[57] Morgan RJ, O'Neal JE. ACS Org Coatings Plastics Prepr 1974; 34:195.
[58] Struik LCE. Physical aging in amorphous polymers and other materials, Amsterdam: Elsevier, 1978.
[59] Zoller P, Hoehn HH. J Polym Sci B: Polym Phys 1982;20:1385.
[60] Li H-L, Ujihira Y, Nanasawa A, Jean YC. Mater Sci Forum 1997;255–7:399.
[61] Robertson CG. PhD thesis, Virginia Polytechnic Institute and State University, Blacksburg, 1999.